Fabrication of SnO$_2$ by RF magnetron sputtering for electron transport layer of planar perovskite solar cells

R Thanimkan[1]**, B Namnuan**[2] **and S Chatraphorn**[1,3] *

[1]Physics of Energy Materials Research Unit, Department of Physics, Faculty of Science, Chulalongkorn University, Phyathai Rd., Bangkok 10330, Thailand
[2]Department of Physics, Faculty of Science, Silpakorn University, Nakhon Pathom 73000, Thailand
[3]Thailand Center of Excellence in Physics, CHE, 328 Si Ayutthaya Rd., Bangkok 10400, Thailand

* Corresponding author's e-mail: Sojiphong.C@chula.ac.th

Abstract. The requirements of electron transport layer (ETL) for high efficiency Perovskite solar cells (PSCs) are, for example, appropriate band energy alignment, high electron mobility, high optical transmittance, high stability, and easy processing. SnO$_2$ has attracted more attention as ETL for PSCs because it has diverse advantages, e.g., wide bandgap energy, excellent optical and chemical stability, high transparency, high electron mobility, and easy preparation. The SnO$_2$ ETL was fabricated by RF magnetron sputtering technique to ensure the chemical composition and uniform layer thickness when compared to the use of chemical solution via spin-coating method. The RF power was varied from 60 - 150 W. The Ar sputtering gas pressure was varied from 1×10^{-3} - 6×10^{-3} mbar while keeping O$_2$ partial pressure at 1×10^{-4} mbar. The thickness of SnO$_2$ layer decreases as the Ar gas pressure increases resulting in the increase of sheet resistance. The surface morphology and optical transmission of the SnO$_2$ ETL were investigated. It was found that the optimum thickness of SnO$_2$ layer was approximately 35 - 40 nm. The best device shows J$_{sc}$ = 27.4 mA/cm^2, V$_{oc}$ = 1.03 V, fill factor = 0.63, and efficiency = 17.7%.

1. Introduction

Perovskite is the next generation of photovoltaic devices because it has achieved high power conversion efficiency (PCE). The PCE has been evolved from 3.8 % to more than 23 % in less than 10 years. The fabrication process is also relatively simple. The normal structure of PSCs consists of five layers, i.e., transparent electrode (FTO or ITO), electron transport layer (ETL), perovskite absorber layer, hole transport layer (HTL), and metal electrode [1]. The requirements of ETL for high efficiency PSCs are (i) appropriate energy band alignment, (ii) high electron mobility, (iii) high optical transmittance, and (iv) high stability and easy processing [2]. The ETLs that have been proposed for PSCs are, for example, TiO$_2$, ZnO, SnO$_2$, etc. TiO$_2$ is usually used for ETL as a compact layer and a mesoporous layer. Both layers give relatively higher efficiency PSCs. However, TiO$_2$ layer has some limitations for PSCs such as it needs high temperature process and yields low electron mobility. The effect of TiO$_2$ layer negatively affects the device stability under ultraviolet (UV) illumination. In addition, ZnO is another choice of ETL. It can be deposited easily with low temperature process. However, ZnO is environmentally unstable due to the hydroxide (OH) residue on the ZnO surface causing the decomposition of perovskite layers. Recently, SnO$_2$ has attracted great attentions as an ETL for PSCs because it has diverse

advantages, e.g., wide bandgap energy (3.6 - 4.0 eV), excellent optical and chemical stability, high transparency, high electron mobility (~ 240 cm^2/Vs), and easy preparation [3-4]. In this work, we demonstrated normal planar structure of PSCs with optimized room-temperature-processed SnO_2 as ETL prepared by spin-coating and RF magnetron sputtering process [5-7]. Two types of process were investigated and found that the devices based on SnO_2 film by RF magnetron sputtering showed superior performance. We considered the effects of RF sputtering parameters such as RF power, Ar and O_2 gas pressure in the performance of PSCs.

2. Experimental

2.1. Preparation of SnO₂ films

The 3 cm × 3 cm fluorine-doped tin oxide (FTO) substrates were etched with Zn powder and HCl for transparent electrode. The FTO substrates were ultrasonically cleaned with detergent (Micro 90), deionized (DI) water, acetone, and 2-propanol (IPA) for 30 min, respectively. The surface treatment of the FTO substrates were done by UV-ozone for 10 min prior to the deposition of ETL. In this work, SnO_2 films as ETL were prepared by spin-coating and RF magnetron sputtering techniques. For spin-coating, the SnO_2 film was deposited using $SnCl_4.5H_2O$ dissolved in IPA (0.15 M), as seen in figure 1 (a). The SnO_2 film was spin-coated at 3000 rpm for 40 s and then annealed on a hotplate at 200 °C for 60 min in air. For RF sputtering technique, Ar and O_2 gas were used during sputtering process as shown in figure 1 (b). RF sputtering power was varied from 60 - 150 W and the Ar sputtering gas pressure was varied from 1×10^{-3} - 6×10^{-3} mbar while keeping O_2 partial pressure at 1×10^{-4} mbar.
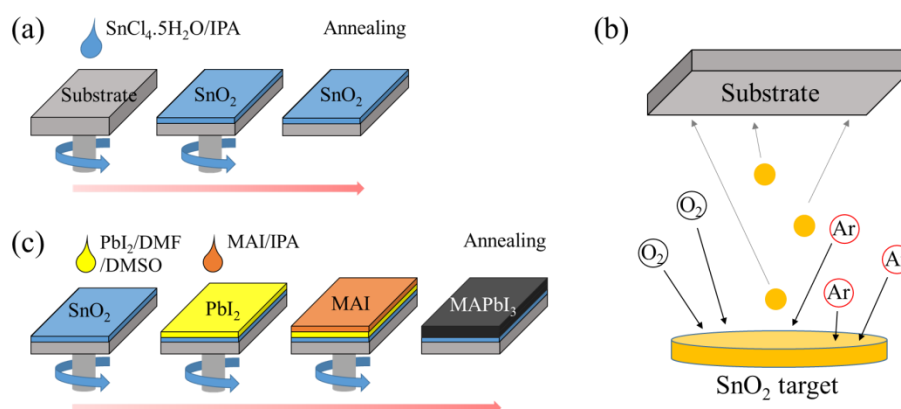

Figure 1. (a) spin-coating method of SnO_2 films, (b) RF magnetron sputtering deposition process, and (c) two-step spin-coating method to deposit $MAPbI_3$ perovskite films.

2.2. Device fabrication

The SnO_2 film was treated by UV-ozone for 10 min to improve its hydrophilicity. The methylammonium lead iodide ($MAPbI_3$ or $CH_3NH_3PbI_3$) perovskite thin film was deposited by the two-step spin-coating method in N_2-filled glovebox as shown in figure 1 (c). The PbI_2 solution was prepared from 0.461 g PbI_2 dissolved in 1 ml of DMF (N,N-Dimethylformamide) and DMSO (N,N-Dimethylsulfoxide) with 4:1 by volume and stirred at 70 °C for 12 hrs. Before depositing perovskite layer, the SnO_2 substrates were preheated on a hotplate at 70 °C for 10 min. The PbI_2 solution was deposited on the preheated SnO_2 by spin-coating at 3000 rpm for 30 s, and then annealed on a hotplate at 70 °C for 20 min. After that, the solution of methylammonium iodide (MAI) was spin-coated on the PbI_2 layer at 2000 rpm for 20 s, which consists of 0.010 g MAI dissolved in 1 ml of IPA and stirred for 12 hrs. In order to obtain a high quality perovskite absorber layer, the anti-solvent technique was employed while spin-coating the MAI layer. All the perovskite layers were annealed on a hotplate at 120 °C for 10 min. The HTL was deposited on top of the perovskite layer using Spiro-OMeTAD solution by a spin-coating at 3000 rpm for 30 s, which was prepared by dissolving 0.0723 g of Spiro-OMeTAD into 1 ml chlorobenzene (CB) and 28.8 µl of 4-tert-butylpyridine (t-BP) and 17.5 µl of lithium bistrifluoromethanesulfonimidate (Li-TFSI) (pre-

dissolved as 520 mg/ml solution in acetonitrile). It was worthy to note that the perovskite absorber layer and HTL process were carried out inside the N_2-filled glovebox. Finally, the Au metal electrode was deposited on the HTL by thermal evaporation.

2.3. Characterization

The surface morphology of the SnO_2 and perovskite films was investigated using a field-emission scanning electron microscopy (FESEM, JEOL Model JSM-7001F). The transmittance and absorbance spectra were investigated in the range of 330 - 1100 nm by a UV-Vis-NIR spectrophotometer (Shimadzu Model UVPC1600). The J-V curves of the PSCs were measured under AM 1.5 using a Xe-lamp solar simulator and a Keithley 238 source-meter unit. The PSC devices under investigation have an active area of 0.06 and 0.2 cm^2.

3. Results and discussion

3.1. Spin-coated SnO_2 films

The morphology of SnO_2 film deposited on soda-lime glass (SLG) substrates by spin-coating method is shown in figure 2 (a). The SnO_2 films can fully cover the SLG substrates. However, it can be seen that when SnO_2 precursor was deposited by spin-coating method, some particulates from recrystallization of $SnCl_4$ precursor was obtained on some area of SnO_2 surface. Figure 2 (b) shows the J-V curves of the best PSC by spin-coating of SnO_2 film measured under both forward and reverse voltage scan directions. The PCE was about 12.9 % and the open-circuit voltage (V_{oc}), the short-circuit current density (J_{sc}), and the fill factor (FF) of the best device are 1.04 V, 18.4 mA/cm^2, and 0.68, respectively. The J-V curves show some slight hysteresis between forward and reverse directions.
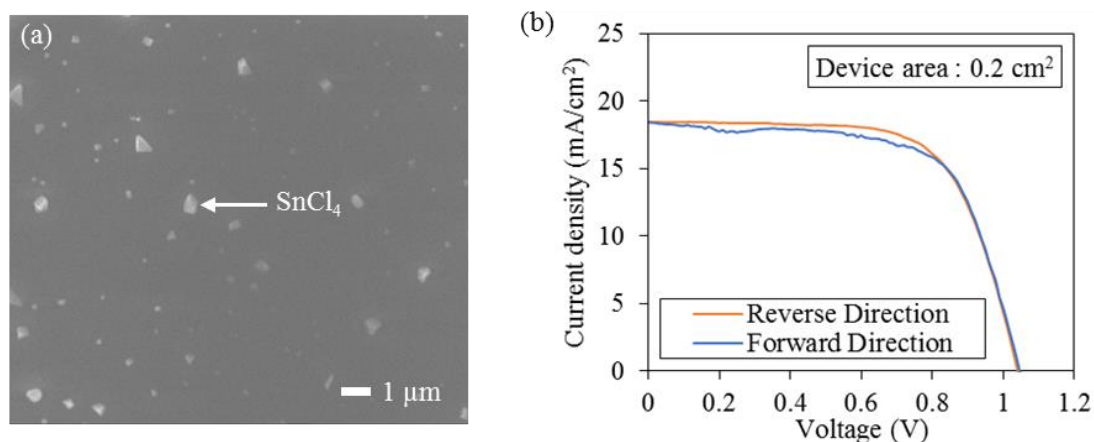

Figure 2. (a) SEM image shows surface morphology of spin-coated SnO_2 film on SLG substrates. (b) J-V curves of the best PSC based on spin-coated SnO_2 film measured under forward and reverse voltage scans.

3.2. Sputtered SnO_2 films

SEM image of surface morphology of sputtered SnO_2 film on SLG substrates shows very smooth surface as shown in figure 3 (a), The cross-section of a complete PSC is shown in figure 3 (b). The J-V curves of four conditions are compared for the sputtered SnO_2 films under various RF sputtering power of 60, 90, 120 and 150 W. It is shown in the J-V curves in figure 4 (a) that the performance of PSCs become worse with increasing RF sputtering power. Table 1 summarizes the photovoltaics parameters of PSCs with different sputtering power. The best device was obtained with 60 W RF sputtering power with champion PCE of 17.7 %, V_{oc} of 1.03 V, J_{sc} of 27.4 mA/cm^2, and fill factor of 0.63.
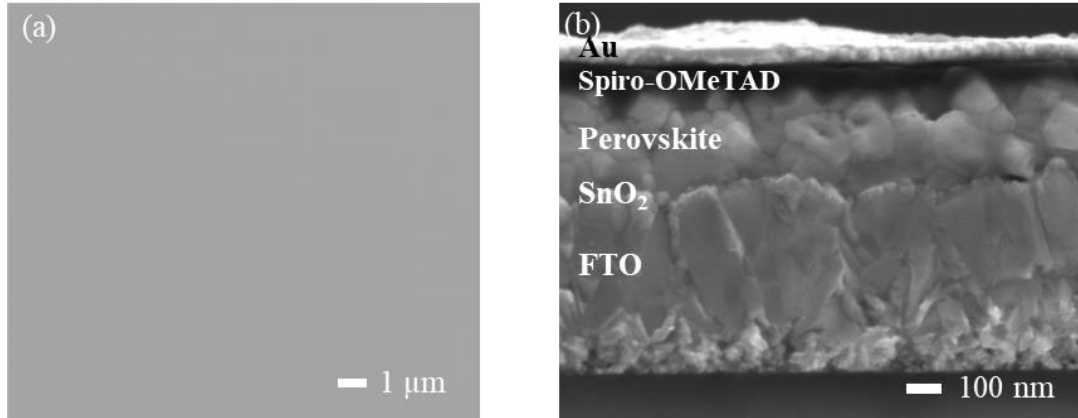
Figure 3. SEM image shows (a) smooth surface morphology of sputtered SnO_2 film on SLG substrate, and (b) cross-section of a complete PSC.
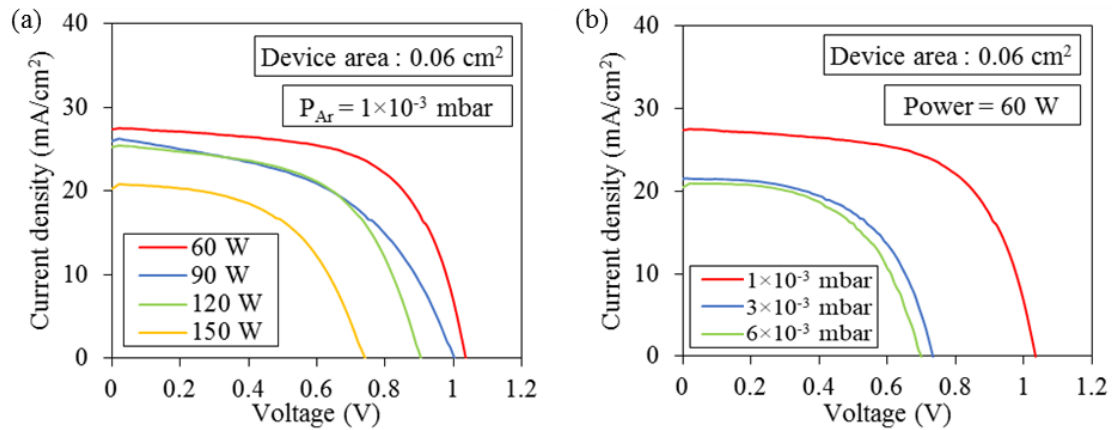

Figure 4. J-V curves of PSCs based on sputtered SnO_2 film; (a) with different RF sputtering power, and (b) RF sputtering power of 60 W at different Ar gas pressures while keeping O_2 gas pressure.

Table 1. The solar cell parameters of PSCs based on different RF sputtering power of sputtered SnO_2 film.

RF power (W)	V_{oc} (V)	J_{sc} (mA/cm^2)	Fill factor	PCE (%)
60	1.03	27.4	0.63	17.7
90	1.00	26.0	0.50	12.9
120	0.90	25.2	0.57	12.9
150	0.74	20.3	0.55	8.2

In order to investigate the effect of Ar sputtering gas pressure on the device performance. The complete devices were fabricated on the sputtered SnO_2 films under various Ar gas pressure (1×10^{-3}, 3×10^{-3}, and 6×10^{-3} mbar) while keeping O_2 gas pressure at 1×10^{-4} mbar. As shown in figure 4 (b), with decreasing the Ar gas pressure, the device performance was gradually improved. The optical transmission of the sputtered SnO_2 films were greater than 85% in the range of solar spectrum as shown in figure 5. The best device was obtained when the Ar gas pressure was 1×10^{-3} mbar, showing high $V_{oc} = 1.03$ V, $J_{sc} = 27.4$ mA/cm^2, fill factor = 0.63, and PCE of 17.7 %. The detailed photovoltaics parameters were listed in table 2. The increase in Ar gas pressure results in the decrease of mean free path, leading to the increase in the deposition time to achieve the optimum thickness about $35 - 40$ nm. In addition, decreasing the thickness of SnO_2 layer corresponded to increasing of sheet resistance.
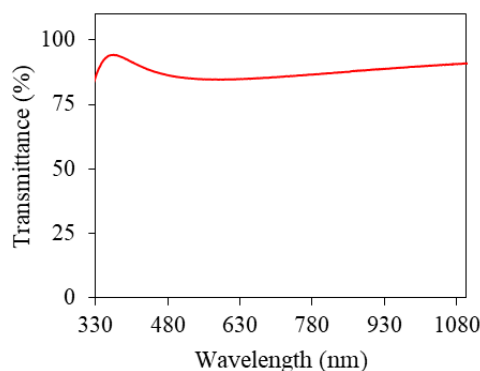
Figure 5. Optical transmission spectrum of the sputtered SnO_2 film.

Table 2. Photovoltaic parameters of PSCs with sputtered SnO_2 ETL with different Ar gas pressure.

Ar pressure(mbar)	V_{oc} (V)	J_{sc} (mA/cm^2)	Fill factor	PCE (%)
1×10^{-3}	1.03	27.4	0.63	17.7
3×10^{-3}	0.74	21.0	0.58	9.0
6×10^{-3}	0.70	20.5	0.56	8.0

4. Conclusion

SnO_2 films for use as an ETL layer in planar PSCs were fabricated and compared for the performance of PSCs employing SnO_2 films by spin-coating and RF magnetron sputtering techniques. It was found that sputtered SnO_2 based devices were demonstrated to have better device performance and stability than spin-coated SnO_2 based devices. Wet chemical processes were avoided to minimize the particulates from recrystallization of SnO_2 precursor. This also leads to uneven surface of the ETL layer. It can also be observed that improper sputtering parameters strongly affect the V_{oc}, J_{sc} and thus the PCE. In this work, the PSC based on sputtered SnO_2, with the RF sputtering power of 60 W and Ar gas pressure of 1×10^{-3} mbar with O_2 gas partial pressure of 1×10^{-4} mbar showed champion PCE of 17.7 %.

References

[1] Lee J and Park N 2015 *MRS Bull.* **40** 654–9
[2] Jiang Q, Zhang X and You J 2018 *Small* **14** 1801154
[3] Xiong L, Guo Y, Wen J, Liu H, Yang G, Qin P and Fang G 2018 *Adv. Funct. Mater.* **28** 1802757
[4] Yi H, Wang D, Mahmud M, Haque F, Upama M, Xu C, Duan L and Uddin A 2018 *ACS Appl. Energy Mater.* **1** 6027–39
[5] Kam M, Zhang Q, Zhang D and Fan Z 2019 *Sci. Rep.* **9** 6963
[6] Bai G, Wu Z, Li J, Bu T, Li W, Huang F, Zhang Q, Cheng Y and Zhong J 2019 *Sol. Energy* **183** 306–14
[7] Otoufi M, Renjbar M, Kermanpur A, Taghavinia N, Minbashi M, Forouzandeh M and Ebadi F 2020 *Sol. Energy* **208** 697–707